minerals

MDPI

Article

Organic and Isotopic Geochemistry of Evaporites and Shales of the Santana Group (Araripe Basin, Brazil): Clues on the Evolution of Depositional Systems and Global Correlation during the Lower Cretaceous

Naedja Vasconcelos Pontes [1], Daniel Bezerra das Chagas [2], Ana Clara Braga de Souza [3], Daniel Rodrigues do Nascimento Junior [4,*], Wellington Ferreira da Silva Filho [4], Ramsés Capilla [5], Antônio Jorge Vasconcellos Garcia [6] and José de Araújo Nogueira Neto [2]

1 Federal Institute of Education, Science and Technology of Piauí (IFPI), Paulistana 64750-000, Piauí, Brazil; naedjapontes@ifpi.edu.br
2 Faculty of Science and Technology (FCT), Federal University of Goiás (UFG), Aparecida de Goiânia 74968-755, Goiás, Brazil; dchagas@ufg.br (D.B.d.C.); jose.araujo@ufg.br (J.d.A.N.N.)
3 Geology Graduate Program (PPGG), Federal University of Ceará (UFC), Fortaleza 60440-554, Ceará, Brazil; anaclarageologia@alu.ufc.br
4 Department of Geology, Federal University of Ceará (UFC), Fortaleza 60440-554, Ceará, Brazil; welfer@ufc.br
5 Geochemistry Laboratory of the Petrobras Research Center (CENPES), Leopoldo Américo Miguez de Mello Research and Development Center, Petrobras S.A., Rio de Janeiro 21941-915, Rio de Janeiro, Brazil; capilla@petrobras.com.br
6 Department of Geology, Federal University of Sergipe, São Cristóvão 49100-000, Sergipe, Brazil; garciageo@hotmail.com
* Correspondence: daniel.rodrigues@ufc.br

Citation: Pontes, N.V.; das Chagas, D.B.; de Souza, A.C.B.; do Nascimento Junior, D.R.; da Silva Filho, W.F.; Capilla, R.; Garcia, A.J.V.; de Araújo Nogueira Neto, J. Organic and Isotopic Geochemistry of Evaporites and Shales of the Santana Group (Araripe Basin, Brazil): Clues on the Evolution of Depositional Systems and Global Correlation during the Lower Cretaceous. *Minerals* **2021**, *11*, 795. https://doi.org/10.3390/min11080795

Academic Editor: Krzysztof Bukowski

Received: 11 June 2021
Accepted: 17 July 2021
Published: 22 July 2021

Abstract: Even being the more studied of the interior basins of Northeast Brazil, the Araripe Basin still lacks research in organic geochemistry designed to support interpretations of depositional systems and conditions of formation. This work aims to investigate the organic behavior of evaporites and shales from the Santana Group (Lower Cretaceous), as well as discuss their role in the evolution of its depositional systems. A total of 23 samples, 17 shales and six evaporites, were collected in outcrops and quarries. Analyses of Total Organic Carbon (TOC), Total Sulfur (TS), Rock Eval pyrolysis, and the $\delta^{34}S$ isotope ratio were performed. The TOC results revealed high organic content for seven intervals, of which only five had high TS content. From the Rock Eval pyrolysis, dominance of the Type I kerogen was verified, thus corresponding to the best type of organic matter (mainly algal) for the generation of liquid and gaseous hydrocarbons. The Lower Cretaceous (probably Aptian) response to the progressive evolution in redox conditions is linked to a remarked Oceanic Anoxic Event (OAE-1a). The TOC/TS ratio suggests variable palaeosalinity, indicating most of the shales were formed under brackish waters with saline influence, yet tending to increase the salinity upwards where hypersaline conditions dominate in the Ipubi Formation. The isotope data also suggest the occurrence of marine ingressions in the depositional systems even prior to the well-documented event of the Romualdo Formation.

Keywords: geochemistry; evaporites; paleosalinity; sulfur isotope; TOC/TS ratio; Cretaceous Oceanic Anoxic Event; marine ingression; Batateira Bed; Araripe Basin

1. Introduction

In ancient sedimentary basins, evaporites can record climatic, physiographic, environmental, and hydrochemistry changes. In this regard, some studies debate the marine or nonmarine origin for these sedimentary deposits (e.g., [1–5]). However, some evaporites show evidence of having formed from a mixture of open-ocean water and waters that record a continental influence (cf. [6]). In such a transitional environment, evaporites may

be associated with a semi-enclosed basin that becomes progressively isolated and were deposited under brackish-saline conditions, such that its sedimentological and geochemical characteristics become increasingly influenced by oceanic inputs [7–9]. In this environment, some geochemical evidence suggests that salinity conditions may be due to influxes of seawater during brief marine connections and lake transgression [10].

The sulfur cycle in an aquatic system would help to discriminate among a mix of possible paleoenvironments from transitional settings, thus unraveling eventual marine incursion events towards coastal waterbodies [10–12]. Since fluctuations in the sulfur isotope composition play a role in many natural processes, the knowledge of its content and composition characteristics can enhance the understanding of various geological processes [13–15]. Particularly, in sedimentary basins, the deposition of organic matter and sulfur may reflect changes in physical, chemical, and biological conditions through chemoclines in the water column [16–20]. Besides that, the geochemical research suggests that the sulfur isotopic composition could reconstruct fluctuations in the base level of sedimentary environments [11,21,22].

In addition, the geochemical behavior of evaporites and shales can be related to other processes such as the bacterial sulfate reduction and total organic carbon (TOC) increase. For its turn, these processes may be related to anoxic conditions with abundant organic matter as a reductant that couples sulfur with carbon. Previous studies have proposed several mechanisms to reconstruct fluctuations in the sedimentary environment using this approach. Recent geochemical researches attest that the anomalous sulfur isotopic composition in marine sediments can be crucial to paleoredox chemical conditions [18,23], but relevant papers focusing on the effect of redox conditions in the sulfur isotopic signals from the Araripe Basin is still scarce [18,23–28].

Globally, the Aptian interval (late Lower Cretaceous) is a widely investigated timespan based on the paleo-oceanographic, paleoenvironmental, and paleoclimatic changes, globally recorded in the sedimentary rock successions. The Aptian documents the influence of environmental changes, such as relative sea-level fluctuations, variations in sea surface temperature, type and intensity of detrital influx, and the impact of variations in the carbon cycles associated with global oceanic anoxic events [29–35]. In this context, the Santana Group in the Araripe Basin (Brazil) covers successions from the Upper Aptian (the local Alagoas Stage), corresponding to a "post-rift" sequence [27,28,36]. This group is famous not only locally, due to extensive limestone and gypsum deposits, but also worldwide for its rich paleontological content, preserved in limestones and carbonate concretions [37–39], both considered truly fossil *konservat lagerstaetten* [40–42].

This study aimed to investigate the geochemical characteristics from the Santana Group and the paleoenvironmental signatures of its evaporites and shales. Both lithologies can contribute to understand the factors regulating the paleoredox chemical conditions, yet being useful to reconstruct changes in the depositional systems of the unit. This will also be of value in answering the debated question of whether marine incursions contributed to the organic carbon accumulation inside the Santana Group.

2. Geological Setting

The Araripe Basin (Figure 1), located in northeastern Brazil, was generated from tec-tonic events associated with the break-up of the West Gondwana paleocontinent and the opening of the modern Southern and Equatorial Atlantic Ocean [43]. The structural framework of the basin is linked to the reactivation of Precambrian basement structures, posteriorly favoring the opening of intracontinental rifts aborted from the Brazilian Northeast Rift System [44–46]. A transitional phase, amid the rift and the early post-rift (post-rift I) phases in the Araripe Basin, encompass the Barbalha, Crato, Ipubi, and Romualdo formations that compound the Santana Group [36]. These formations show a complex tectonic-sedimentary evolution formed by the stacking of several stratigraphic sequences limited by unconformities of regional nature [36,47]. Besides that, this succession also

involves an interval recording a complete transgressive-regressive cycle, limited at the base by a pre-Aptian unconformity [46,48].

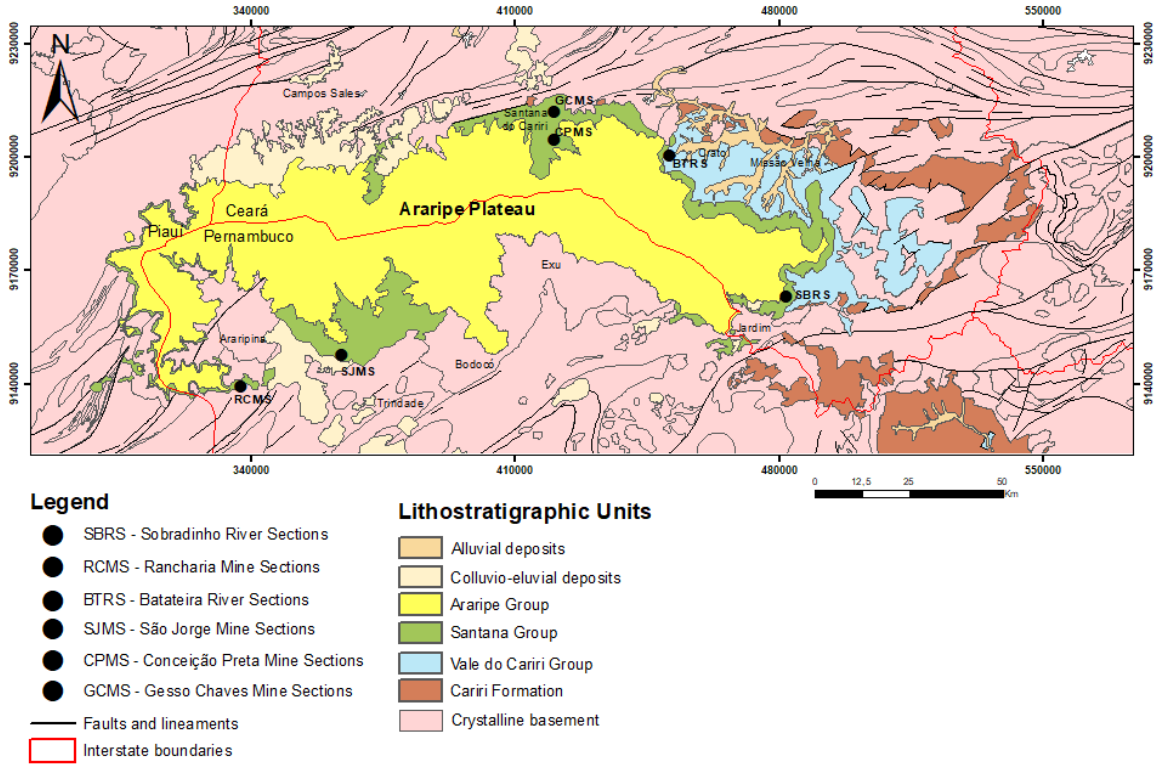

Figure 1. Geological map of the study area depicting the Araripe Plateau with the indication of major lithostratigraphic units and structural features. The black circles localize the Batateira River (BTRS), Sobradinho River (SBRS), Rancharia Mine (RCMS), São Jorge Mine (SJMS), Gesso Chaves Mine (GCMS), and Conceição Preta Mine (CPMS) sections analyzed in this research.

The Santana Group, according to lithostratigraphic nomenclature propositions from Neumann and Cabrera (2002) [49], Assine et al. (2014) [36], and Neumann and Assine (2015) [47], involve laminated limestones, gypsum evaporites, sandstones, carbonate concretions, mudstones, siltstones, pelites, and dark shales [36,50]. At the base of this group, the Barbalha Formation occurs intercalating sandstones and shales, but also including black shales of the Batateira Bed, a highlighted stratigraphic marker that Hashimoto et al. (1987) [51] initially proposed as an organic-rich immature source rock. Overlying the Barbalha Formation are the Crato Formation, a unit which has an approximate thickness of 70 m [48]. This formation is composed predominantly of limestones with planar and parallel laminations containing widespread *Dastilbe crandalli* fish fossils [52–54], but also alternating shales between the limestone intervals. Some specific intervals inside the limestones are rich in famous, diverse, and exceptionally well-preserved fossils (i.e., [55]). Recent studies carried out on the Craton Formation have proposed a microbial nature for its limestones [56,57].

Discontinuous evaporite beds of the Ipubi Formation are deposited right above the Crato Formation and consist of gypsum-rich successions, interpreted as associated with coastal sabkhas [48] or a playa lake system [58]. Lastly, the Romualdo Formation is the uppermost lithostratigraphic unit of the Santana Gr. being mainly composed of shales, which is also recognized worldwide by its superb preservation of fossils inside carbonate concretions present in some levels (e.g., [59–62]). In a recent work, Custódio et al. (2017) [63] described a transgressive-regressive cycle in the Romualdo Formation in which the fossil-bearing black shale would mark a maximum flooding surface. As a whole, the Santana

Group is bounded by an unconformity at its top with the alluvial Araripina and Exu formations [36].

3. Materials and Methods

3.1. Samples

A total of six evaporite samples and 17 shale samples from the Santana Group were analyzed and interpreted in this study. The lateral correlation of the samples was made through six columnar sections, exhibiting the stratigraphic position of the rocks (Figure 2). The samples were collected along stratigraphic sections denominated Batateira River (BTRS), Sobradinho River (SBRS), Rancharia Mine (RCMS), São Jorge Mine (SJMS), Gesso Chaves Mine (GCMS), and Conceição Preta Mine (CPMS) (Figures 1 and 2). The shale samples are dominated by dark green, gray, and black lithics, whereas evaporite samples were mainly white luster, massive gypsum layers (Figures 2 and 3); both rocks were directly selected from outcrops and quarries in the sections. The samples belong to the same collecting sites of the work from Chagas (2017) [64,65], who collect them originally for facies and palynologic purposes.

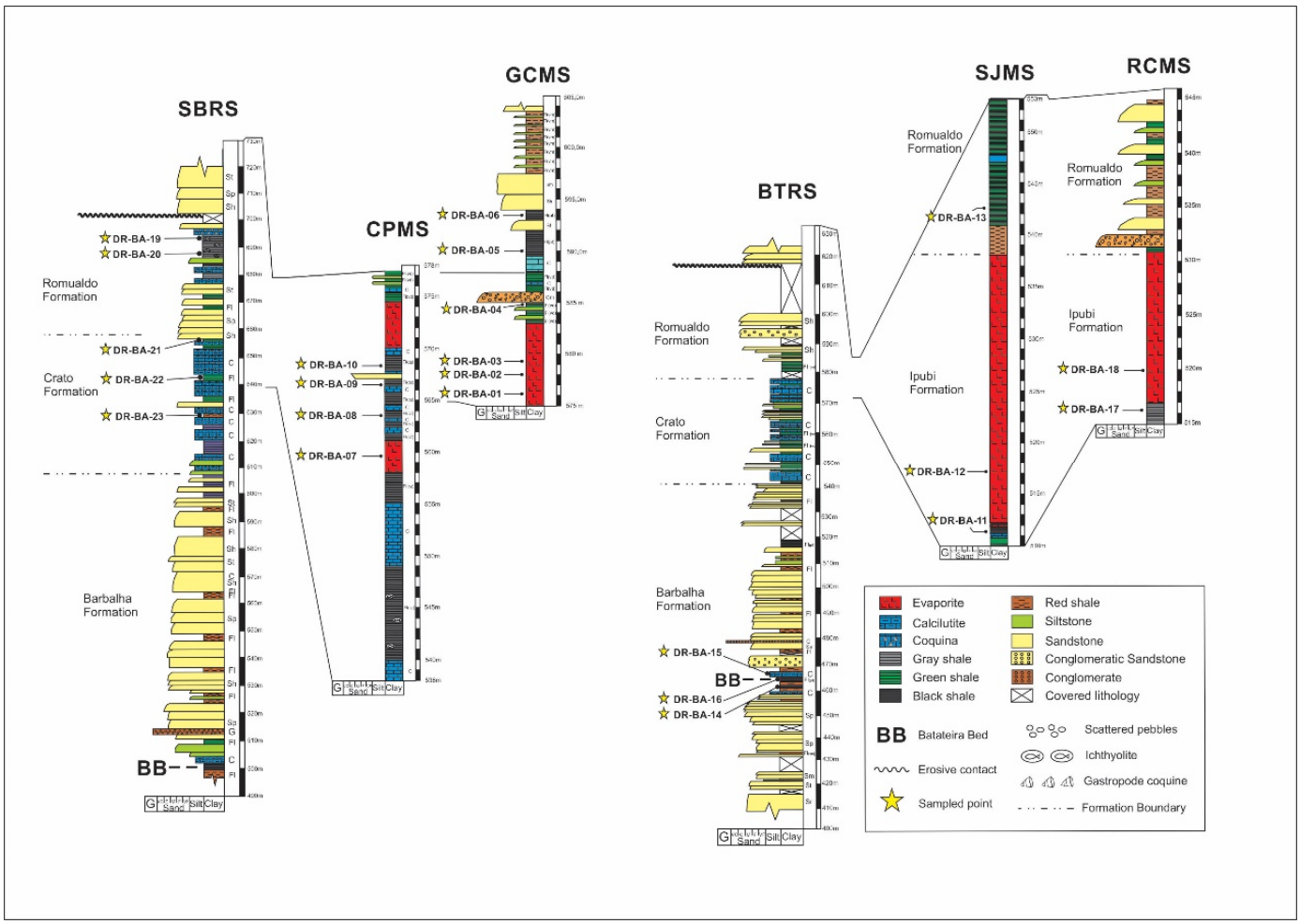

Figure 2. Columnar sections of the Santana Group formations, including facies, thickness, position of collected samples, and lateral correlation. The abbreviation means the name of the sections analyzed in this research: Batateira River (BTRS), Sobradinho River (SBRS), Rancharia Mine (RCMS), São Jorge Mine (SJMS), Gesso Chaves Mine (GCMS), and Conceição Preta Mine (CPMS).

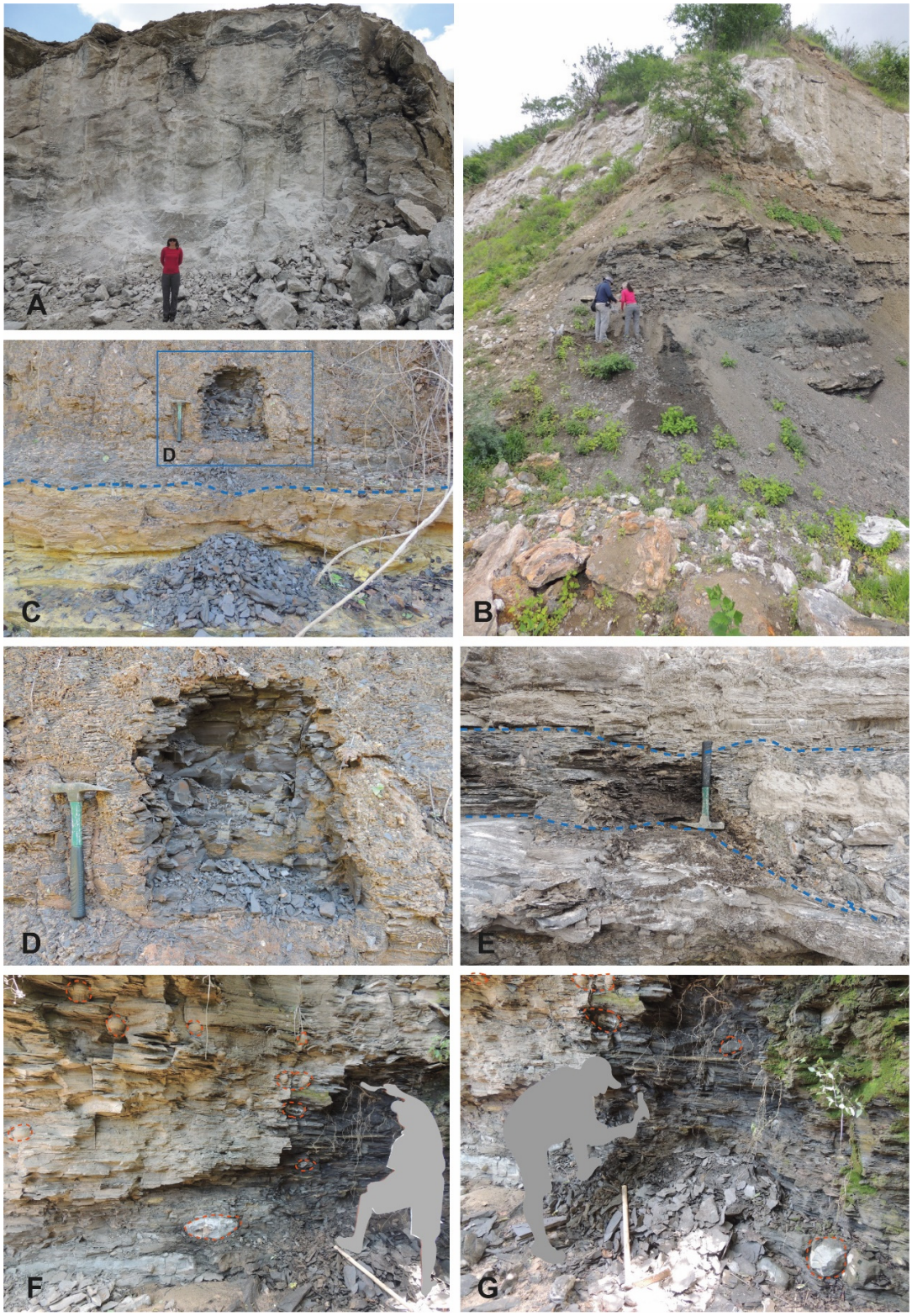

Figure 3. Outcrops of the evaporites and shales collected in the study sections and main features of the lithofacies. (**A**) Evaporite from the São Jorge Mine (SJMS). (**B**) Black shales from the Conceição Preta Mine section (CPMS). (**C**) A transition between limestone and a sampled shale. (**D**) Detail on where the sample DR-BA-10 (CPMS) was collected. (**E**) Crato Formation shale sample (DR-BA-22) located between carbonate beds from the Sobradinho River section (SBRS). (**F**) Detail on nodular carbonate concretions from the Sobradinho River's shale (Romualdo Formation). (**G**) Detail on where the sample DR-BA-19 was collected in the Sobradinho River section (SBRS).

The dataset obtained from the shale samples include total organic carbon content (TOC), total sulfur content (TS), Rock-Eval Pyrolysis index (RE), and isotopic ratios of sulfur ($\delta^{34}S_{V\text{-}CDT}$). For the evaporite samples, only the isotopic analysis of sulfur was performed. All analyses were made at the Geochemistry Laboratory of the Leopoldo Américo Miguez de Mello Research and Development Center (CENPES) of Petrobras.

3.2. Methods

3.2.1. TOC and TS

The determination of total sulfur contents in rocks by itself does not provide detailed information, being generally evaluated in conjunction with TOC data, thus providing valuable subsidies to the interpretation of the depositional environment in which the rock was formed [66], and can be interpreted in terms of paleosalinity of the depositional system.

Initially, an aliquot of 250 g of each shale sample was crushed and then sieved with an 80-mesh sieve. Then, the powdered samples were reacted with 32% hydrochloric acid to eliminate eventual inorganic carbon from carbonates. After this, the samples were washed with distilled water to remove traces of HCl. The samples were also dried in an oven at 60°C and, after cooling, total organic carbon and sulfur were measured. The reliability of all the selected samples were tested before measuring the carbon-sulfur analyses using a LECO-SC144DR device.

3.2.2. Rock-Eval Pyrolysis

For the analysis of the source rock potential through pyrolysis, samples that yielded TOC contents lower than one weight percent (1 wt%) were discarded, following the recommendation of [67]. Only seven samples provided TOC values higher than 1% and thus have pyrolysis analyses. The four parameters obtained from the pyrolysis were: The amount of free hydrocarbons present within the sample (S1 curve, mg HC/g rock), hydrocarbons generated from the cracking of kerogen (S_2 curve, mg HC/g rock), Tmax (thermal maturity proxy, calculated from the temperature peak of the S_2 curve, in °C), and carbon dioxide (CO_2) released during the analyses (S_3 values, CO_2/g rock). These parameters followed the method described by Espitalié et al. (1977) [68]. During analysis, the samples were heated under an inert atmosphere of helium. This technique was performed in a flame ionization detector sensitive to organic compounds emitted during three heating steps, while sensitive infrared detectors measured CO and CO_2 during pyrolysis and oxidation [69].

Additionally, two other derived parameters were calculated: The hydrogen index (HI) or hydrogen to carbon ratio (H/C), that is equal to (S_2/TOC) × 100, and the oxygen index (O/I) or oxygen to carbon ratio (O/C), that is equal to (S_3/TOC) × 100 [70]. The HI and OI furnish an estimation of the organic matter type by indicating the type of kerogen present within the sample, being posteriorly plotted on a Van Krevelen diagram. A classic differentiation of the type of organic matter (kerogen types I, II, and III) follows the proposal by Tissot and Welte (1978) [71].

3.2.3. Sulfur Isotope Analysis

Among the 17 initial samples of shale, six presented less than 0.01% of total sulfur, which is insufficient for sulfur isotopic analysis. For the remaining 11 shale samples, as well as for the six evaporite samples, the sulfur isotopic ratios ($^{34}S/^{32}S$) were measured in a Finnigan Mat 252 mass spectrometer. The sulfur isotopic values here are reported in $\delta^{34}S$ in parts per mill (‰) of deviation relative to the established Vienna Canyon Diablo troilite standard (V-CDT) (IAEA standard S-1). The analytical precision of the method is ±0.2‰ for $\delta^{34}S$.

4. Results and Interpretations

Rock-Eval parameters (HI and OI), total organic carbon (TOC), sulfur content (TS), and the bulk organic sulfur isotopic composition ($\delta^{34}S$) of a sample give valuable clues on the type of kerogen, the maturity of the organic matter present, the salinity, and oxygenation.

The location and vertical position of the collected samples of the Santana Group are shown in Figures 1 and 2, while Table 1 exhibits the analytical results of geochemical and isotopic analysis of them.

Table 1. Total sulfur (TS), total organic carbon (TOC), hydrogen index (HI), oxygen index (OI), and sulfur isotopic ($\delta^{34}S$) values obtained for the investigated lithotypes. The vertical stacking is in agree with the stratigraphic positioning of the collected samples.

Formation (Shale/Evaporite)	Sample	TS (%)	TOC (%)	HI (mg HC/g TOC)	OI (mg CO_2/g TOC)	$\delta^{34}S$ V-CDT (‰)
Romualdo (S)	DR-BA-19	1.25	5.65	272.74	14.34	−10.06
Romualdo (S)	DR-BA-20	0.97	3.92	678.06	30.61	−9.83
Romualdo (S)	DR-BA-06	0.01	0.11	-	-	-
Romualdo (S)	DR-BA-05	0.17	1.03	151.46	39.81	−9.6
Romualdo (S)	DR-BA-04	0.77	0.01	-	-	−12.85
Ipubi (E)	DR-BA-03	-	-	-	-	+16.90
Ipubi (E)	DR-BA-02	-	-	-	-	+16.94
Ipubi (E)	DR-BA-01	-	-	-	-	+16.51
Ipubi (E)	DR-BA-07	-	-	-	-	+16.95
Ipubi (S)	DR-BA-10	1.07	0.73	-	-	−15.45
Ipubi (S)	DR-BA-09	0.52	1.04	146.15	28.85	−10.92
Ipubi (S)	DR-BA-08	0.55	0.09	-	-	−13.03
Ipubi (S)	DR-BA-13	0.01	0.03	-	-	-
Ipubi (E)	DR-BA-18	-	-	-	-	+17.71
Ipubi (E)	DR-BA-12	-	-	-	-	+17.11
Ipubi (S)	DR-BA-11	1.8	10.2	740.59	14.80	−16.18
Ipubi (S)	DR-BA-17	3.41	23.3	736.91	17.77	−16.36
Crato (S)	DR-BA-21	0.01	0.69	-	-	-
Crato (S)	DR-BA-22	0.01	0.72	-	-	-
Crato (S)	DR-BA-23	0.01	0.34	-	-	-
Barbalha (S)	DR-BA-15	1.3	13.7	648.69	32.48	−13.35
Barbalha (S)	DR-BA-16	0.11	0.71	-	-	−5.27
Barbalha (S)	DR-BA-14	0.04	0.64	-	-	-

4.1. Chemostratigraphic Units

Five chemostratigraphic units, named A to E, were defined for the studied interval from the TOC, insoluble residue (IR), and TS geochemical data, as shown in Figure 4. In the following section, Figure 4 presents a detailed description.

4.1.1. Unit A

The lowermost chemostratigraphic unit (Figure 4) includes the lower half of the Barbalha Fm., from its ordinary basal gray shales to the black shales of the Batateira Bed. This interval is equivalent to the so-called "first fluvial cycle"—i.e., Assine 2007 [48], believed to encompass riverine braided systems gradually replaced by a lacustrine establishment at the top. The unit A is characterized by TOC values ranging from 0.4% to 13.7%, total sulfur from 0.04 to 0.11, and insoluble residue (IR) from 31% to 89%. All terrigenous shale samples presented insoluble residue values above 70%, while lower values were found in calcitic shales. In particular, the Batateira Bed shows a high content of total organic carbon (13.7%), total sulfur of 1.3%, and insoluble residue of only 31%, the lowest among all samples.

4.1.2. Unit B

The second unit is highlighted by low values of TOC (between 0.34% and 0.72%) and total sulfur (0.01%) (Figure 4). The presence of carbonates in the insoluble residue is noted only in the sample DR-BA-22 (calcitic shale), as characterized in the section studied by Chagas (2017) [65], where there is a gradual transition from black shales to finely laminated gray to cream colored limestones from the Crato Formation.

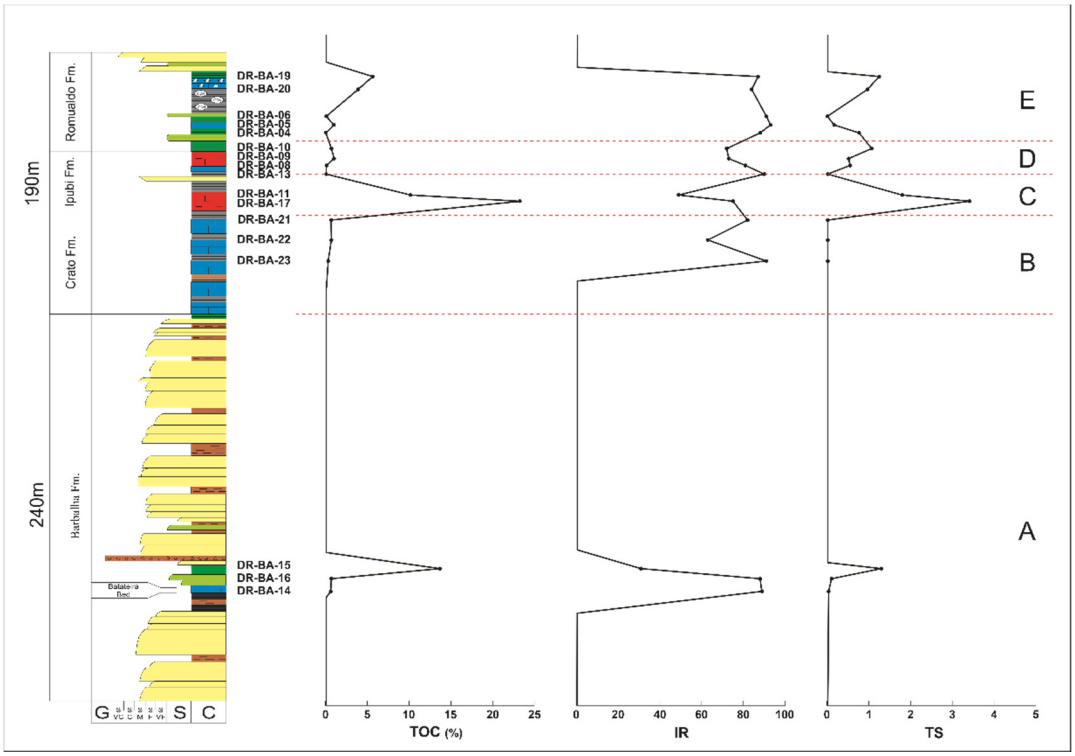

Figure 4. Vertical variation of total organic carbon (TOC), insoluble residue (IR), and total sulfur (TS) from samples of the Santana Group. Five chemostratigraphic units (**A**–**E**) are highlighted between the dashed lines. See the text for explanation.

4.1.3. Unit C

The third chemostratigraphic unit presents two high TOC (10.2% and 23.3%) and total sulfur (1.8% and 3.41%) values in the samples DR-BA-11 and DR-BA-17, coinciding with the lower evaporite layer of the Ipubi Fm. (Figure 4). Soon above, unit C reaches low values of TOC and TS of 0.01% and 0.03% respectively, both nearby the upper evaporite layer of the Ipubi Fm.

4.1.4. Unit D

The unit D exhibits an oscillation of high and low values in TOC contents from 0.09% to 1.04% (Figure 4), where the shale sample DR-BA-09 is potentially a source rock for hydrocarbons, having been collected at the base of the upper evaporite layer of the Ipubi Fm.

4.1.5. Unit E

The topmost unit starts with almost zero total sulfur values at the base, then progressively increases towards the top (Figure 4). At the same time, TOC ranges from 0.09% to 1.04% at the base and with a significant increase to the top. The samples at the top are DR-BA-20 (3.92% TOC and 0.97% total sulfur) and DR-BA-19 (5.65% TOC and 1.25% total sulfur), being shales of the Romualdo Fm.

4.2. Relationship between Total Organic Carbon and Total Sulfur

The TOC of the analyzed shales presented values between 0.01% and 23.3%, while the sulfur values ranged from 0.01% to 3.41% (Table 1). Based on analyses of numerous samples from ancient and recent depositional systems, Berner and Raiswell (1983) [72] and Leventhal (1995) [73] concluded the existence of a good linear correlation between organic carbon and sulfur (in the form of sulfide) contents in fine sediments, from which it would be possible to discriminate the paleosalinity of waters of the depositional systems into hypersaline, saline, and fresh. According to Raiswell (1984) [74], under anoxic conditions,

bacteria promote the reduction of sulfates, having H_2S as one of the products; if detrital iron is available, it reacts to H_2S, then generating sedimentary pyrite. In the case of seawater, this contains a larger amount of dissolved sulfates, and therefore, in a marine environment, the formation of sedimentary pyrite would be greater than in freshwater environments. This interpretation, however, requires great caution because it compares marine depositional systems in terms of salinity, whose relationship is not always straightforward in continental systems (i.e., oxygenated, endorheic/evaporitic lakes).

Paleosalinity variations are also interpreted by Woolfe et al. (1995) [75], based on the calculation of the C/S ratio, where they synthesized the method so that the parameters also apply to oxygenated waters: 1.5–4.0 (normal marine salinity); 4.0–11.0 (brackish with saline influence); 11.0–17.0 (brackish with freshwater influence); more than 17.0 (freshwater environment). In combination with the total organic carbon content of this research, the total sulfur content was deposited partly under anoxic conditions, whose C/S ratio is classified in Figure 5.

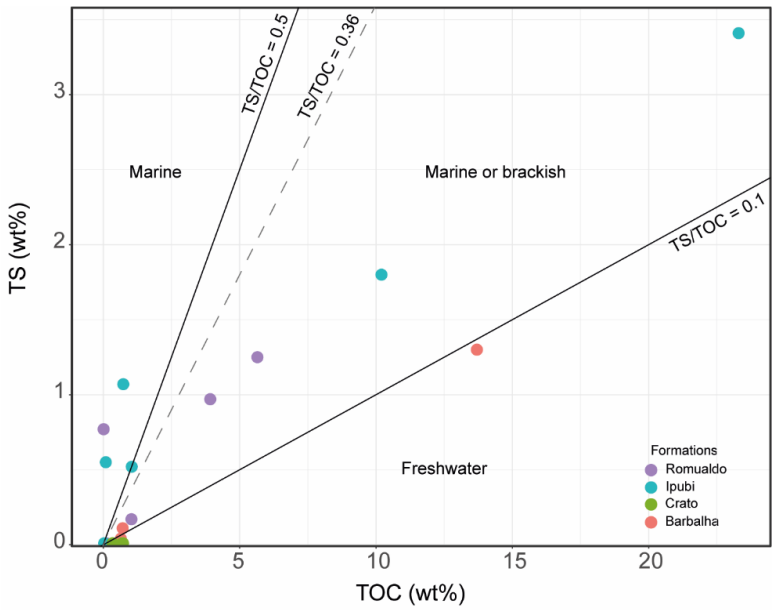

Formation	Samples	C/S Ratio	Paleosalinity
Romualdo	DR-BA-04	0.01	-
Romualdo	DR-BA-05	6.06	Brackish with saline influence
Romualdo	DR-BA-06	11.00	Brackish with saline influence
Romualdo	DR-BA-19	4.52	Brackish with saline influence
Romualdo	DR-BA-20	4.04	Brackish with saline influence
Ipubi	DR-BA-08	0.16	-
Ipubi	DR-BA-09	2.00	Normal sea salinity
Ipubi	DR-BA-10	0.68	-
Ipubi	DR-BA-11	5.67	Brackish with saline influence
Ipubi	DR-BA-13	3.00	Normal sea salinity
Ipubi	DR-BA-17	6.83	Brackish with saline influence
Crato	DR-BA-21	69.00	Freshwater influence
Crato	DR-BA-22	72.00	Freshwater influence
Crato	DR-BA-23	34.00	Freshwater influence
Barbalha	DR-BA-14	16.00	Brackish with freshwater influence
Barbalha	DR-BA-15	10.54	Brackish with saline influence
Barbalha	DR-BA-16	6.45	Brackish with saline influence

Figure 5. Total sulfur (TS) vs. total organic carbon (TOC) plot (after Leventhal, 1995 [73]) and the C/S ratio (after Woolfe et al. 1995 [75]) to interpret paleosalinity of the Santana Group.

Usually, low TOC values indicate that little or no organic matter is being preserved and suggest oxic conditions [66]. In the other hand, different sub-environments in the

depositional systems can develop dominantly anoxic conditions when the input rate of degradable organic matter exceeds oxygen diffusion, so the oxygen can be depleted at the water-sediment interface of water bodies with restricted circulation. Significant anoxic events such as OAE's (Oceanic Anoxic Events) consist of global episodes favoring organic carbon deposition and preservation [76] as a response on oceanic variations, i.e., reduced oxygenation level, sea-level rise, etc. Several models suggest even episodic causes for these events, such as restriction of paleogeographic environments relative to the oceans, stagnation of oceanic currents, increased continental surface runoff, abnormally high organic productivity, and intense and widespread deep-sea volcanic activity [77]. In the continental domain, anoxic conditions are more geographically restricted and may occur in lacustrine systems or those bearing flooded soils [78], such as floodplains of riverine systems.

The Barbalha Fm. is traditionally interpreted as being formed by two fluvial cycles finalized by dominantly lacustrine systems, the first of which ended in the Batateira Bed [48]. In this work, one sample from the first fluvial cycle falls within the field interpreted as brackish with freshwater influence, suggesting that arid conditions early began to reach the fluvial system of Barbalha Fm.; however, the overlying samples (including the Batateira Bed) fall into the brackish conditions with saline influence. For the Batateira Bed, the TOC and TS values are high (13.7% and 1.3%, respectively), suggesting an origin possibly related to a moment of maximum flooding, whose base level elevation would have contributed to anoxia in the system. There, a mild increase in the salinity could come from more arid conditions and/or invasion by marine waters.

In the Crato Fm., which is to date interpreted as a lacustrine system due to its fossiliferous association in the laminated limestones and an apparent absence of marine clues [48], the samples of shale fall within the context of a freshwater environment, with low TOC (<0.72%) and total sulfur (<0.1%) contents. Shales and limestones are the main rocks occurring interdigitated in the Crato Fm., whose paleogeography is thought to be a fragmented lacustrine system for most of the unit's history, rather than a single large lake, as the shales are formed under relatively shallower water than the limestones, and are also more abundant towards the basin boundaries [47,49]. There is evidence of aridity reached in the limestone layers, such as halite pseudomorphs [41]; however, the vertical stacking of limestones passing to shales demonstrate that moments of lacustrine spatial restriction occurred. Since the interlayered shales were precisely the rocks sampled in the present study, there is still a chance that the climate was possibly wetter in these intervals. In this case, one possibility for the result of the present study would be the presence of fresher and shallower lake waters, which in the latter respect would still facilitate circulation under more oxidizing conditions at the bottom.

In the Ipubi Fm, the shales occur with results indicating normal marine salinity and brackish salinity with marine influence, matching similar conditions of the evaporites in the same unit. In lakes, the variation in salinity is generally related to their depth: The deeper and more stratified the lake, the higher the salt concentration in the hypolimnion [79]. Water salinity also intensely influences the abundance and variety of organisms in lake ecosystems, decreasing the primary productivity as the salinity increases [80]. However, extremely-high salinity (hypersalinity) invariably relates to high temperature due to more intense evaporation [81] and a higher saturation of salts in a relatively smaller aqueous volume. Samples collected at Nova Olinda (north of the basin) suggest more saline conditions than those collected at Araripina and Trindade (south of the basin), suggesting more significant restriction and/or effective evaporation from endorheic waters in the northern portions.

Finally, at Romualdo Fm., the samples suggest sedimentation in conditions with C/S ratios strongly variable, from low to high values, i.e., with abrupt salinity increment, which may have facilitated the mortality of freshwater fishes recorded exactly at the place where fossiliferous carbonate concretions (ichthyolites) are found [82,83]. Notwithstanding, the association of carbonate-pelitic lithofacies of the Romualdo Formation also preserved

fossil fishes tolerant to high saline conditions, being in the deeper strata the mixed haline genus *Calamopleurus* [38], and in the more superficial ones some frankly marine genera like *Rhacolepis* and *Vinctifer* [84].

4.3. Organic Matter Type

The study of kerogen types positioned the analyzed samples dominantly between the fields of Types I and III of organic matter (Figure 6), then encompassing freshwater algal and marine or lacustrine planktonic origin but also humic organic matter, derived from terrestrial plants [68]. Samples with Type I kerogen (DR-BA-11, DR-BA-17, DR-BA-20, and DR-BA-15) would thus have the best type of organic matter for liquid and gaseous hydrocarbon generation. In contrast, samples with Types II and III kerogens (DR-BA-05, DR-BA-09, and DR-BA-19) would comprise samples with lower potential in hydrocarbon generation.

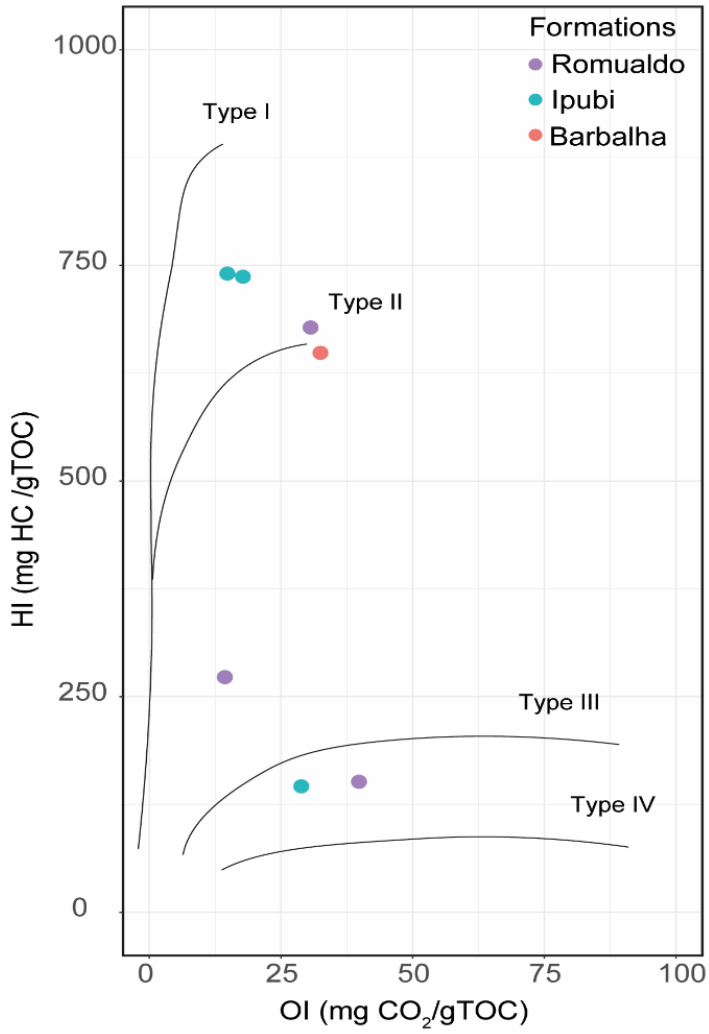

Figure 6. Crossplot of the oxygen index (OI) versus hydrogen index (HI) (Van Krevelen diagram) for classifying the kerogen types of the Santana Group. The shales of the Crato Formation do not present significant content in organic matter for this analysis (Table 1). The discriminant fields are following Espitalié et al. (1977) [68].

4.4. Sulfur Isotopic Clues

The results of the sulfur isotopic analysis ($\delta^{34}S_{V\text{-}CDT}$) are shown in Table 1 and Figure 7 where the samples of shale showed a variation from −16.36‰ to −5.27‰ and those of evaporite from +16.51‰ to +17.71‰.

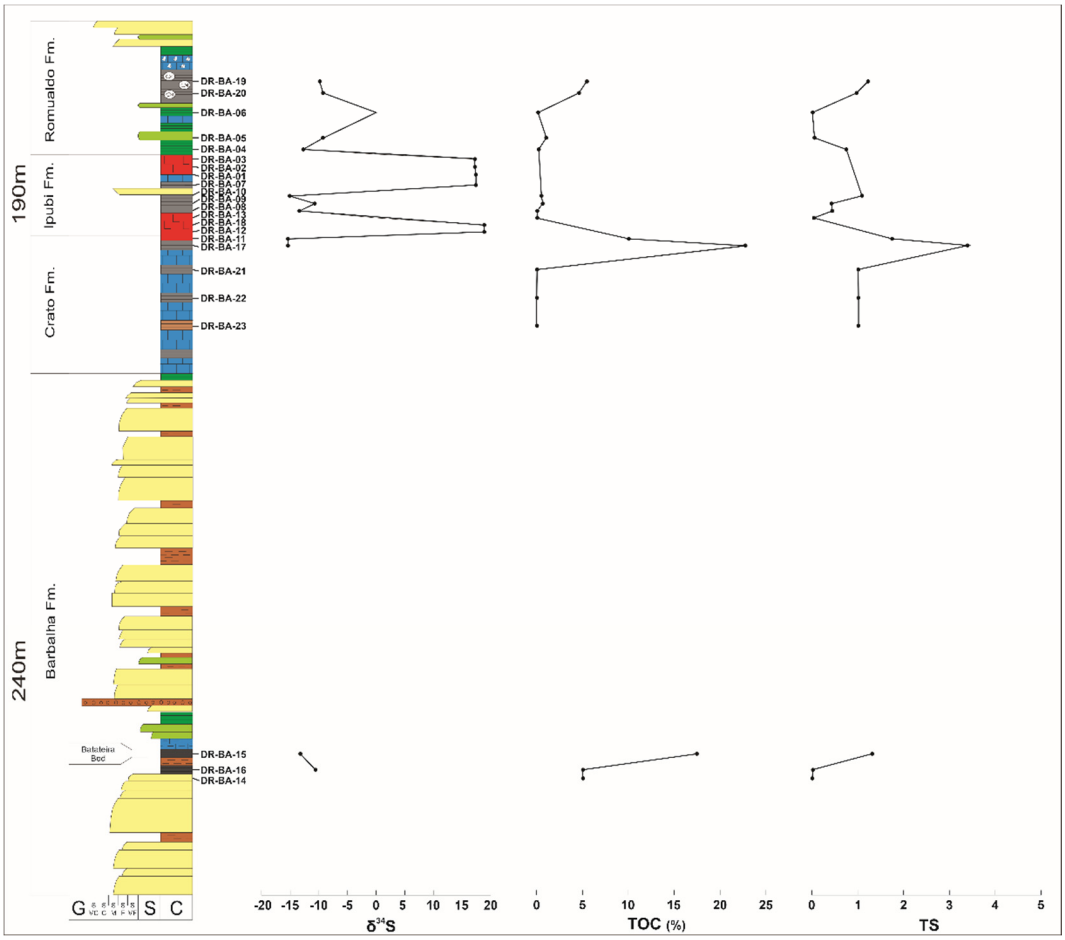

Figure 7. Compared variations between sulfur isotope ($\delta^{34}S$), total organic carbon (TOC), and total sulfur (TS) values from samples of the Santa Group. See text for explanation.

The highest TOC values in this analysis were interpreted to be positioned at maximum flooding surfaces (MFS) within the Santana Group, which would be marked in three possible anoxic events associated with environmental changes over a relatively short time interval. Assine et al. (2014) [36] assumed three MFSs inside the Santana Group based on the gamma-ray of well profiling that coincides with the MFSs of the present research. These flooding surfaces also match with the boundaries of the so-called "Depositional Sequence 1" (DS-1), "Depositional Sequence 2" (DS-2), and "Depositional Sequence 3" (DS-3) of that study [36]. The contact between DS-1 and DS-2 is positioned on the marly shales of the Batateira Bed, while the contact between DS-2 and DS-3 is positioned on the evaporitic section of the Ipubi Fm. Inside the DS-3, the flooding surface was positioned in the upper portion of a dominantly transgressive system tract succession, in this case, the shales with fossiliferous concretions at the level of bioclastic limestones of the Romualdo Fm.

The Batateira Bed showed an isotopic value of −13.35‰, a value typical of a lacustrine system; negative values like this indicate that much of the existing sulfur is of bacterial origin, favoring enrichment in the light isotope (^{32}S). Farina (1974) [85] named the Batateira Bed as a "plumbiferous sequence" due to a mineralization in lead, zinc, and copper sulfides that generally associate with an intermediate lens of limestone or marl inside the unit. Therefore, it is believed that hydrogen sulfide has been produced by bacterial reduction under anaerobic conditions. It may have been fixed in the sediment as pyrite and as organic sulfur. For Rios-Netto et al. (2012) [86], the combined lithological and palynological features, including the presence of *Botryococcus* algae, indicate deposition in a shallow lacustrine environment, also arguing that none marine palynomorphs were found. The shale immediately below the Batateira Bed resulted in a $\delta^{34}S_{V\text{-}CDT}$ of −5.27‰; in this

case, one possibility is that the environment was more oxygenated and with a decreasing influence of anaerobic bacterial activity. In the Crato Fm., the samples obtained low total sulfur results (0.01%), making $\delta^{34}S_{V\text{-}CDT}$ isotopic analysis impossible for the used method.

There is no consensus on the depositional system for the origin of the evaporites of Ipubi Fm. In his early research, Lima (1978) [87], based on micropaleontological association, positioned the formation in a transitional environment, arguing that there is no evidence for the existence of a broad marine basin nor an exclusively continental system. For its turn, Arai and Coimbra (1990) [88] detected the presence of a fossiliferous assembly composed of pollen, spores, dinoflagellates, ostracods, foraminifera, and mollusks typical of coastal environments with "unquestionable" marine influence. Soon after, Assine (1992) [89] interpreted the unit as formed in arid coastal systems of a supratidal realm (sabkha) exposed to sea-level variations. More recently, Nascimento et al. (2016) [58], based on facies, petrography, mineralogy, and chemical analyses, have hypothesized the possibility of a playa lake-like system subject to salinity oscillations and perhaps surface hydrothermalism, but with no marine connection.

Geochemically, sulfate is comparatively abundant in seawater, which is why the zone of sulfur-reducing bacteria is extensive, and the sulfate concentration in lakes is lower [78]. The isotopic results for all evaporite samples in this study indicated enrichment in the heavy isotope (^{34}S, with $\delta^{34}S_{V\text{-}CDT}$ values of +16.51‰ to +17.71‰), and a value of approximately 1‰ higher was noticeable in samples of the Ipubi Fm. collected southwards in the Pernambuco State when compared to those collected in Ceará (this work), demonstrating that sulfate reduction was higher in the latter region. It is known that the similarity between $\delta^{34}S$ values of sulfate minerals and dissolved sulfate in seawater indicates that the mineralogy is a good proxy for the depositional conditions of the brines [90,91]. The $\delta^{34}S_{V\text{-}CDT}$ values of the gypsum from the studied samples are in agree with the normative values recorded by Claypool et al. (1980) [90] for Cretaceous evaporites (+13‰ to +20‰) interpreted as marine, then suggesting a marine water influence in the evaporites of the Ipubi Fm. based on its isotopic signature (Figure 8). For the modern ocean, the isotopic value of $\delta^{34}S$ is between +20‰ and +21‰ [91,92].

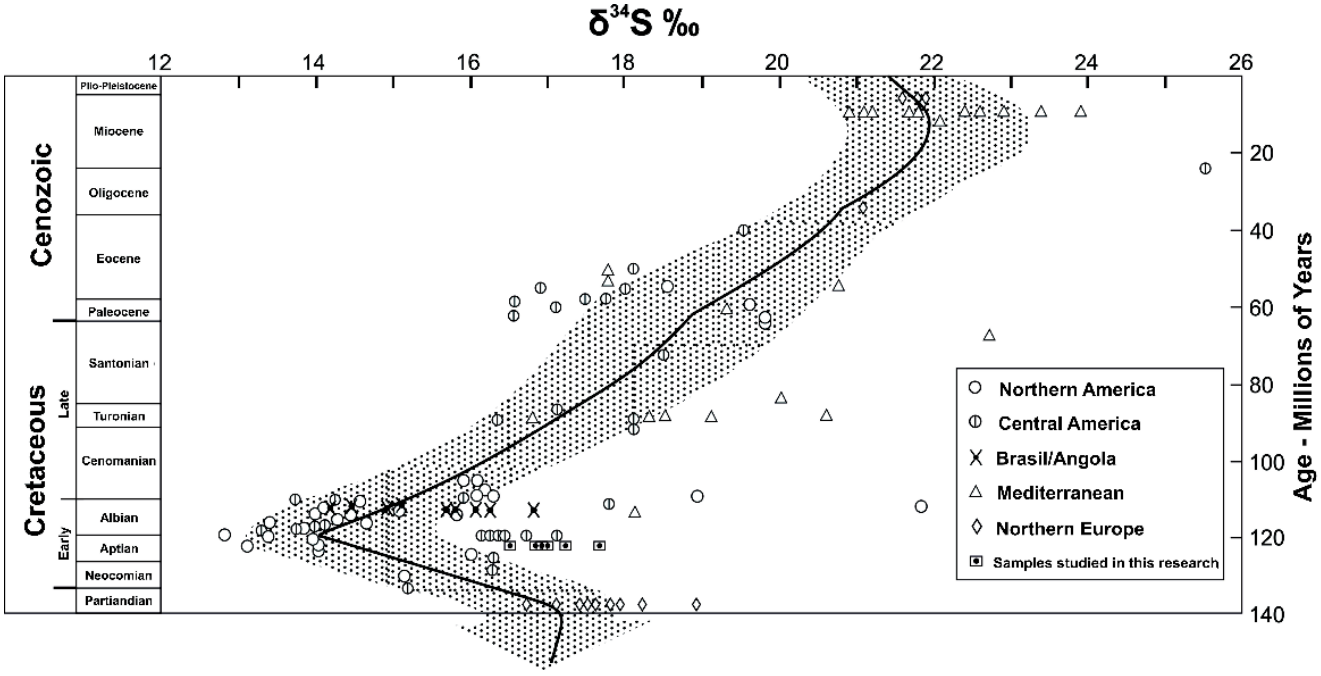

Figure 8. Global curve of sulfur isotopic variations in marine evaporites from the Cretaceous modified from Claypool (1980) [90]. Data from North America, Central America, Brazil/Angola (only from the coastal basins), Mediterranean, Northern Europe, and this research.

The reduction of sulfate generates a kinetic effect on sulfur isotope fractioning, causing the hydrogen sulfide generated to be depleted in the heavy isotope ^{34}S [93]. For Bottrell and Newton (2006) [94], this happens due to the predilection of bacteria for the lighter isotope. Therefore, the composition of sedimentary sulfides would reflect the chemical, isotopic composition of hydrogen sulfide produced during sulfate reduction [95]. Studies by Fry et al. (1991) [96] and Neretin et al. (1998) [97] show that sulfides in sediments or waters under euxinic conditions are commonly depleted in ^{34}S with a range of −45‰ to −70‰ relative to seawater sulfate.

In the present study, the compared isotopic results of evaporites and shales of the Ipubi Fm. are contrasting, being enriched in ^{34}S in the first case and depleted in the second case. This situation indicates that this depletion of the heavy isotope in the shales is associated with the dissimilatory reduction of sulfate by bacteria that is balanced by the enrichment of ^{34}S in the water sulfate (generator of the evaporites). In periods of high biological activity by sulfate-reducing bacteria, there is an increase of the ^{34}S value in the waters (and their evaporites), especially in the oceans, due to the preferential removal of ^{34}S-depleted sulfur as sedimentary sulfides [91]. This would explain the significantly negative values for the shales situated at the base of the evaporites in contrast to the isotopic values of the evaporites themselves, thus suggesting an isotopic signature of marine composition. The isotopic values for the evaporites in this research are within the range of +10.27‰ to +17.99‰ found by Barros et al. (2016) [98] and Bobco et al. (2017) [26], where they interpreted evaporitic subaqueous systems with seawater mixing at times, and also a marine origin for the brine generating the evaporitic deposits, respectively.

In the Romualdo Formation, the $\delta^{34}S$ isotopic results of the shales located just above the second (last) evaporite layer of the Ipubi Formation were −12.85‰ (DR-BA-04) and, soon above, −9.6‰ (DR-BA-05). Thus, there is a slight enrichment of the ^{34}S isotope even when compared to the shales from beneath the evaporites. This enrichment could be influenced by a mixing of waters (marine and lacustrine). It is known that several forms of dinoflagellates were recognized in the shales just above the gypsum of the Ipubi Formation [87]. Arai and Coimbra (1990) [88] also recognized dinoflagellates of the genera *Subtilisphaera* and *Spiriferites*, suggesting marine influence in their depositional environment. Importantly, Chagas (2017) [65] identified groups of marine palynomorphs (i.e., *Rodonascia bontei*) at the same stratigraphic levels of this research in both the base and top shales of the Ipubi Formation, ratifying marine ingressions, as well as a coincidence with levels with high percentages of the genus *Classopollis*, which are generally associated with deposits near coastal regions. In the case of the sample DR-BA-06, it was not possible to perform $\delta^{34}S$ isotopic analysis because it had an insufficient amount of total sulfur (0.01%), in addition to possibly anoxic conditions (TOC of 0.11%) (Figure 9). However, following towards the top of the Santana Group, two samples were collected in the interval bearing the fossiliferous carbonate concretions, where the isotopic results were −9.83‰ and −10.06‰, implying a slight enrichment in ^{34}S. In this same interval, Chagas (2017) [65] found the dinoflagellate *Subtilisphaera senegalensis*, also considered a marine indicator.

The redox conditions during the deposition of the Santana Group, obtained from the TOC and total sulfur geochemical data, provide constraints on the evolution of the Araripe Basin. These are consistent with previous paleontological and organic biomarker data that indicate saline and redox-stratified conditions in the depositional basin (Figure 9). The Barbalha and Crato formations showed TOC/TS ratios suggesting deposition in a mainly freshwater lacustrine depositional environment, a result in agreement with most of the former research (i.e., [41,102–104]). Usually, the sulfur isotopic data are also consistent with oxic conditions, a finding that also match recent work by Varejão et al. (2021) [105] who interpreted the Barbalha-Crato interval as deposited in a dominantly freshwater lacustrine system due to the abundance of non-marine fossils and an oxygen isotopic ratio ($\delta^{18}O_{V\text{-}PDB}$) between −6.9‰ and −4.48‰.

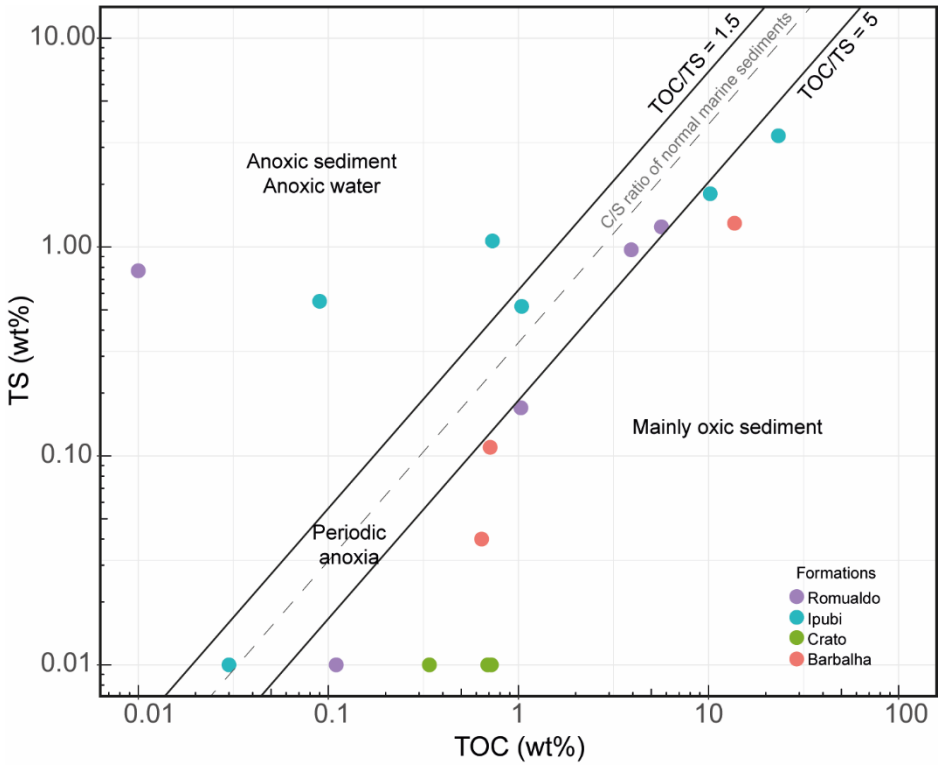

Figure 9. Total sulfur (TS) vs. total organic carbon (TOC) plot for interpreting the paleoredox conditions of the Santana Group. The dashed line represents the average C/S ratio for normal marine sediments (2.8) under oxygenated seawater conditions. Based on Berner [99,100] and Fleurance et al. [101].

Particularly, the Ipubi Formation would represent a regional expansion of anoxic conditions, and most of the studied samples indicate anoxic or periodic anoxic conditions. Besides that, the salinity indicates the transition between brackish waters with saline influence to a water with normal sea salinity. The evaporitic succession is a piece of evidence that the Araripe Basin experienced severe climatic and salinity variations [26,41,57,106]. Recent works [27,107] also point that the evaporites of the Ipubi Formation may have putatively precipitated by the evaporation of marine waters. These findings, as in the present work, point for intermittent marine incursions in the Ipubi Formation [105] rather than an isolated playa-lake environment [58], in a probable true coastal sabkha system [48].

Finally, the Romualdo Formation presents strongly variable signatures of paleoredox conditions (Figure 9), being euxinic conditions with periodic anoxia occurring in samples related to the shale layers with fossiliferous concretions (DR-BA-19 and DR-BA-20), once more pointing to a cause for the mortality recorded in that interval (i.e., [48]), despite not explaining the origin for the (local?) anoxia. The salinity attests for waters under brackish conditions with marine influence (Figure 5). Marine behavior for the Romualdo Formation is well documented (i.e., [48,88]), but only recently have some works gathered evidence for a true epicontinental sea [105,108].

4.5. Global Correlation Based on the Oceanic Anoxic Events

In the Araripe Basin, the Santana Group are recently under debate regarding its chronological positioning inside the Lower Cretaceous [28,109–111], where the traditional view on ages extending into the Albian (Aptian-Albian) is questioned. Despite being studied long ago with microfossils as a basis for correlation [37], the group is still scarce in reliable levels that would be directly correlated with other basins, thus influencing on the precision time-interval of the unit.

Globally well-known oceanic anoxic events (OAE) can be useful in track specific positions inside marine-influenced basins, therefore helping correlation efforts. Once marine flooding events are frequently associated with OAEs, any tools designed to detect this association are useful. In this sense, Assine et al. (2014) [36] recognized three MFSs in the Santana Group, based on gamma-ray data and facies analysis, where at least one global OAEs would be fit based in the time interval. The three MFSs were positioned: i. at the Batateira Bed (inside the Barbalha Fm.); ii. at the base of the Ipubi Fm.; and iii. at the beginning of the final third of the Romualdo Fm. Based on recent works assuming the Ipubi Fm. is deposited in the Late Barremian-Early Aptian interval (126.5–119.5 Ma; [110]) and the Romualdo Fm. as deposited prior the Late Aptian terminus (~113 Ma; [28]), the Selli Event (OEA-1a, ~120 Ma; [112]) would be the only with chances of a record inside the Santana Gr., thus positioned inside the base of the Ipubi Fm. This is coincident with the position where two samples of shale presented the highest TOC and TS values (Table 1, Figure 9) among the overall samples of the Santana Gr.

5. Conclusions

The Santana Group presented, for the analyzed samples of evaporites and shales, high organic richness, with excellent averages of preserved organic matter in seven studied intervals. Three anoxic events would be associated with environmental changes in short time intervals and may correlate with maximum flooding surfaces (MFSs) located in the Barbalha (Batateira Bed), Ipubi, and Romualdo formations. The shales of the Barbalha Fm. showed congruence with freshwater (lacustrine/fluvial), except for the Batateira Bed, with a trend of slightly increased salinity, but still with Type I kerogen (lacustrine algal organic matter) and $\delta^{34}S$ indicative of lacustrine system with significant bacterial activity. Shales from the Crato Formation showed low amounts of TS, making $\delta^{34}S$ analyses impossible; however, their results suggest lacustrine systems in a dominantly freshwater environment. For its turn, Ipubi Formation presented characteristics of an environment rich in saline to hypersaline water, with Type I kerogen and sulfur isotopes relatively enriched in ^{32}S in the shales (due to a reducing bacterial activity) and ^{34}S in the adjacent evaporites, an association suggestive of marine influence. In the Romualdo Formation, half of the samples of shale presented affinity with saline to hypersaline water; moreover, kerogen oscillated between types I and II, and with sulfur isotopic values of −9.83‰ and −10.06‰, and thus may characterize the shales in a depositional system varying from eventually to dominantly-reached by marine water inputs.

The Selli Event (OAE-1a) is the probable global anoxic event recorded inside the Santana Gr., once Ipubi Fm. has clues of marine incursions and the probable age involved fits well. This interpretation reinforces recent publications that consider the entire Santana Gr. as deposited strictly before the Albian in the Lower Cretaceous.

Author Contributions: N.V.P.: Conceptualization, data curation, field activity, sample collection, investigation, formal analysis, visualization, and writing—original draft, review, and editing. D.B.d.C.: Data curation, field activity, sample collection, investigation, formal analysis, and visualization. A.C.B.d.S.: Investigation, formal analysis, visualization, and writing—original draft, review, and editing. D.R.d.N.J.: Supervision, visualization, validation, and writing—review and editing. W.F.d.S.F.: Field planning, field activity, in situ investigation, sample collection review, and editing. R.C.: Laboratory analysis, interpretation. A.J.V.G.: Supervision, visualization, validation, and writing—review and editing. J.d.A.N.N.: Funding, visualization, validation, and writing—review and editing. All authors have read and agreed to the published version of the manuscript.

Funding: This research was supported by the project titled Estratigrafia e paleoecologia de geossítios cretáceos no âmbito do Geopark Araripe (Capes/Funcap ID AE1-0079-000540100/13).

Data Availability Statement: The data presented in this study are available in the text body itself.

Acknowledgments: The authors would like to thank the staff of the Laboratório de Geoquímica (CENPES/Petrobrás) for the geochemical and isotope analyses. We are also grateful to Alexandra Whitbread for the grammar revision, two anonymous referees for the scientific revision on the original

manuscript, and the editorial staff of the journal for the assistance along the submitting process. In particular, N.V.P. and D.B.d.C. acknowledge Fundação Cearense de Apoio ao Desenvolvimento Científico e Tecnológico (Funcap) for their doctorate fellowships.

Conflicts of Interest: The authors declare no conflict of interest.

References

1. Hardie, L.A. Evaporites; marine or non-marine? *Am. J. Sci.* **1984**, *284*, 193–240. [CrossRef]
2. Hardie, L.A. On the Significance of Evaporites. *Annu. Rev. Earth Planet. Sci.* **1991**, *19*, 131–168. [CrossRef]
3. Horita, J.; Zimmermann, H.; Holland, H.D. Chemical evolution of seawater during the Phanerozoic: Implications from the record of marine evaporites. *Geochim. Cosmochim. Acta* **2002**, *66*, 3733–3756. [CrossRef]
4. Hay, W.W.; Migdisov, A.; Balukhovsky, A.N.; Wold, C.N.; Flögel, S.; Söding, E. Evaporites and the salinity of the ocean during the Phanerozoic: Implications for climate, ocean circulation and life. *Palaeogeogr. Palaeoclim. Palaeoecol.* **2006**, *240*, 3–46. [CrossRef]
5. Warren, J.K. Evaporites through time: Tectonic, climatic and eustatic controls in marine and nonmarine deposits. *Earth Sci. Rev.* **2010**, *98*, 217–268. [CrossRef]
6. Denison, R.E.; Kirkland, D.W.; Evans, R. Using Strontium Isotopes to Determine the Age and Origin of Gypsum and Anhydrite Beds. *J. Geol.* **1998**, *106*, 1–18. [CrossRef]
7. Ayora, C.; Taberner, C.; Pierre, C.; Pueyo, J.-J. Modeling the sulfur and oxygen isotopic composition of sulfates through a halite-potash sequence: Implications for the hydrological evolution of the Upper Eocene Southpyrenean basin. *Geochim. Cosmochim. Acta* **1995**, *59*, 1799–1808. [CrossRef]
8. Taberner, C.; Cendón, D.; Pueyo, J.; Ayora, C. The use of environmental markers to distinguish marine vs. continental deposition and to quantify the significance of recycling in evaporite basins. *Sediment. Geol.* **2000**, *137*, 213–240. [CrossRef]
9. Gindre-Chanu, L.; Warren, J.K.; Puigdefàbregas, C.; Sharp, I.R.; Peacock, D.C.P.; Swart, R.; Poulsen, R.; Ferreira, H.; Henrique, L. Diagenetic evolution of Aptian evaporites in the Namibe Basin (south-west Angola). *Sedimentology* **2014**, *62*, 204–233. [CrossRef]
10. Huang, Y.; Yang, G.; Gu, J.; Wang, P.; Huang, Q.; Feng, Z.; Feng, L. Marine incursion events in the Late Cretaceous Songliao Basin: Constraints from sulfur geochemistry records. *Palaeogeogr. Palaeoclim. Palaeoecol.* **2013**, *385*, 152–161. [CrossRef]
11. Holmer, M.; Storkholm, P. Sulphate reduction and sulphur cycling in lake sediments: A review. *Freshw. Biol.* **2001**, *46*, 431–451. [CrossRef]
12. Yücel, M.; Konovalov, S.K.; Moore, T.S.; Janzen, C.P.; Luther, G.W. Sulfur speciation in the upper Black Sea sediments. *Chem. Geol.* **2010**, *269*, 364–375. [CrossRef]
13. Zerkle, A.L.; Kamyshny, A.; Kump, L.R.; Farquhar, J.; Oduro, H.; Arthur, M.A. Sulfur cycling in a stratified euxinic lake with moderately high sulfate: Constraints from quadruple S isotopes. *Geochim. Cosmochim. Acta* **2010**, *74*, 4953–4970. [CrossRef]
14. Johnston, D.T. Multiple sulfur isotopes and the evolution of Earth's surface sulfur cycle. *Earth Sci. Rev.* **2011**, *106*, 161–183. [CrossRef]
15. Pang, Y.; Guo, X.; Shi, B.; Zhang, X.; Cai, L.; Han, Z.; Chang, X.; Xiao, G. Hydrocarbon Generation Evaluation, Burial History, and Thermal Maturity of the Lower Triassic–Silurian Organic-Rich Sedimentary Rocks in the Central Uplift of the South Yellow Sea Basin, East Asia. *Energy Fuels* **2020**, *34*, 4565–4578. [CrossRef]
16. Anderson, T.F.; Pratt, L.M. Isotopic Evidence for the Origin of Organic Sulfur and Elemental Sulfur in Marine Sediments. *ACS Sympos. Ser.* **1995**, 378–396.
17. Suits, N.S.; Wilkin, R. Pyrite formation in the water column and sediments of a meromictic lake. *Geology* **1998**, *26*, 26. [CrossRef]
18. Canfield, D. Biogeochemistry of Sulfur Isotopes. *Rev. Miner. Geochem.* **2001**, *43*, 607–636. [CrossRef]
19. Werne, J.P.; Lyons, T.W.; Hollander, D.J.; Formolo, M.J.; Damste, J.S. Reduced sulfur in euxinic sediments of the Cariaco Basin: Sulfur isotope constraints on organic sulfur formation. *Chem. Geol.* **2003**, *195*, 159–179. [CrossRef]
20. Chen, G.; Chang, X.; Gang, W.; Wang, N.; Zhang, P.; Cao, Q.; Xu, J. Anomalous positive pyrite sulfur isotope in lacustrine black shale of the Yanchang Formation, Ordos Basin: Triggered by paleoredox chemistry changes. *Mar. Pet. Geol.* **2020**, *121*, 104587. [CrossRef]
21. Farquhar, J.; Johnston, D.T.; Wing, B.A.; Habicht, K.S.; Canfield, D.; Airieau, S.; Thiemens, M.H. Multiple sulphur isotopic interpretations of biosynthetic pathways: Implications for biological signatures in the sulphur isotope record. *Geobiology* **2003**, *1*, 27–36. [CrossRef]
22. Canfield, D.; Farquhar, J.; Zerkle, A. High isotope fractionations during sulfate reduction in a low-sulfate euxinic ocean analog. *Geobiology* **2010**, *38*, 415–418. [CrossRef]
23. Kleeberg, A. Interactions between Benthic Phosphorus Release and Sulfur Cycling in Lake Scharmützelsee (Germany). *Water Air Soil Pollut.* **1997**, *99*, 391–399. [CrossRef]
24. Ries, J.B.; Fike, D.; Pratt, L.M.; Lyons, T.W.; Grotzinger, J.P. Superheavy pyrite (34Spyr > 34SCAS) in the terminal Proterozoic Nama Group, southern Namibia: A consequence of low seawater sulfate at the dawn of animal life. *Geology* **2009**, *37*, 743–746. [CrossRef]
25. Yan, D.; Chen, D.; Wang, Q.; Wang, J. Predominance of stratified anoxic Yangtze Sea interrupted by short-term oxygenation during the Ordo-Silurian transition. *Chem. Geol.* **2012**, *291*, 69–78. [CrossRef]
26. Bobco, F.E.R.; Goldberg, K.; Bardola, T.P. Modelo deposicional do Membro Ipubi (Bacia do Araripe, nordeste do Brasil) a partir da caracterização faciológica, petrográfica e isotopica dos evaporitos. *Pesqui. Geociênc.* **2018**, *44*, 431–451. [CrossRef]

27. Goldberg, K.; Premaor, E.; Bardola, T.; Souza, P.A. Aptian marine ingression in the Araripe Basin: Implications for paleogeographic reconstruction and evaporite accumulation. *Mar. Pet. Geol.* **2019**, *107*, 214–221. [CrossRef]
28. Arai, M.; Assine, M.L. Chronostratigraphic constraints and paleoenvironmental interpretation of the Romualdo Formation (Santana Group, Araripe Basin, Northeastern Brazil) based on palynology. *Cretac. Res.* **2020**, *116*, 104610. [CrossRef]
29. Foöllmi, K.B.; Weissert, H.; Bisping, M.; Funk, H. Phosphogenesis, carbon-isotope stratigraphy, and carbonate-platform evolu-tion along the Lower Cretaceous northern Tethyan margin. *Geol. Soc. Am. Bull.* **1994**, *106*, 729–746. [CrossRef]
30. Weissert, H.; Lini, A.; Föllmi, K.B.; Kuhn, O. Correlation of Early Cretaceous carbon isotope stratigraphy and platform drowning events: A possible link? *Palaeogeogr. Palaeoclim. Palaeoecol.* **1998**, *137*, 189–203. [CrossRef]
31. Wissler, L.; Funk, H.; Weissert, H. Response of Early Cretaceous carbonate platforms to changes in atmospheric carbon dioxide levels. *Palaeogeogr. Palaeoclim. Palaeoecol.* **2003**, *200*, 187–205. [CrossRef]
32. Simone, L.; Bravi, S.; Carannante, G.; Masucci, I.; Pomoni-Papaioannou, F. Arid versus wet climatic evidence in the "middle Cretaceous" calcareous successions of the Southern Apennines (Italy). *Cretac. Res.* **2012**, *36*, 6–23. [CrossRef]
33. Westermann, S.; Stein, M.; Matera, V.; Fiet, N.; Fleitmann, D.; Adatte, T.; Föllmi, K.B. Rapid changes in the redox conditions of the western Tethys Ocean during the early Aptian oceanic anoxic event. *Geochim. Cosmochim. Acta* **2013**, *121*, 467–486. [CrossRef]
34. Föllmi, K.B.; Godet, A.; Bodin, S.; Linder, P. Interactions between environmental change and shallow water carbonate buildup along the northern Tethyan margin and their impact on the Early Cretaceous carbon isotope record. *Paleoceanography* **2006**, *21*, 21. [CrossRef]
35. De Souza, A.C.B.; Nascimento, D.R.D.; Filho, F.N.; Batezelli, A.; dos Santos, F.H.; Oliveira, K.M.L.; de Almeida, N.M. Sequence stratigraphy and organic geochemistry: An integrated approach to understand the anoxic events and paleoenvironmental evolution of the Ceará basin, Brazilian Equatorial margin. *Mar. Pet. Geol.* **2021**, *129*, 105074. [CrossRef]
36. Assine, M.L.; Perinotto, J.D.J.; Custódio, M.A.; Neumann, V.H.; Varejão, F.G.; Mescolotti, P.C. Sequências deposicionais do andar Alagoas da Bacia do Araripe, nordeste do Brasil. *Bol. Geociênc. Petrobras* **2014**, *22*, 3–28.
37. Martill, D.M.; Bechly, G.; Loveridge, L.F. *The Crato Fossil Beds of Brazil*; Cambridge University Press: Cambridge, UK, 2007; Volume 1, ISBN 978-0-521-85867-0.
38. Maisey, J.G. *Santana Fossils: An Illustrated Atlas*; TFH Publications Incorporated: Neptune, NJ, USA, 1991; Volume 242, ISBN 978-0-866-225-496.
39. Kellner, A.W.A.; Schobbenhaus, C.; Campos, D.A.; Queiroz, E.T.; Winge, M.; Berbert-Born, M.L.C. Membro Romualdo da Formação Santana, Chapada do Araripe, CE. Um dos mais importantes depósitos fossilíferos do Cretáceo brasileiro. *Sítios Geol. Paleontol. Bras.* **2002**, *1*, 121–130.
40. Martill, D.M.; Bechly, G.; Loveridge, R.F. Introduction to the Crato Formation. *Crato Fossil Beds Braz.* **2009**, 3–7. [CrossRef]
41. Martill, D.M.; Loveridge, R.; Heimhofer, U. Halite pseudomorphs in the Crato Formation (Early Cretaceous, Late Aptian–Early Albian), Araripe Basin, northeast Brazil: Further evidence for hypersalinity. *Cretac. Res.* **2007**, *28*, 613–620. [CrossRef]
42. Martill, D. The age of the Cretaceous Santana Formation fossil Konservat Lagerstätte of north-east Brazil: A historical review and an appraisal of the biochronostratigraphic utility of its palaeobiota. *Cretac. Res.* **2007**, *28*, 895–920. [CrossRef]
43. De Matos, R.M.D.; Krueger, A.; Norton, I.; Casey, K. The fundamental role of the Borborema and Benin–Nigeria provinces of NE Brazil and NW Africa during the development of the South Atlantic Cretaceous Rift system. *Mar. Pet. Geol.* **2021**, *127*, 104872. [CrossRef]
44. Assine, M.L. Sedimentação e Tectônica da Bacia do Araripe, Nordeste do Brasil. Ph.D. Thesis, Universidade Estadual Paulista, Rio Claro, Brazil, 1990.
45. De Matos, R.M.D. The Northeast Brazilian Rift System. *Tectonics* **1992**, *11*, 766–791. [CrossRef]
46. Ponte, F.C.; Ponte Filho, F.C. *Evolução Tectônica e Classificação da Bacia do Araripe*; Report of the Departamento Nacional de Produção Mineral: Recife, Brazil, 1996; p. 68.
47. Neumann, V.H.; Assine, M.L. Stratigraphic proposal to the post-rift I tectonic-sedimentary sequence of Araripe Basin, North-eastern Brazil. In Proceedings of the International Congress on Stratigraphy, Graz, Austria, 19–23 July 2015; Volume 2, p. 274.
48. Assine, M.L. Bacia do Araripe. *Bol. Geociênc. Petrobras* **2007**, *15*, 371–389.
49. Neumann, V.H.; Cabrera, L. Características hidrogeológicas gerais, mudanças de salinidade e caráter endorreico do Sistema lacustre Cretáceo do Araripe, NE Brasil. *Rev. Geolog.* **2002**, *15*, 43–54.
50. Fambrini, G.L.; Silvestre, D.D.C.; Junior, A.M.B.; Da Silva-Filho, W.F. Estratigrafia da Bacia do Araripe: Estado da arte, revisão crítica e resultados novos. *Geol. USP Série Cient.* **2020**, *20*, 169–212. [CrossRef]
51. Hashimoto, A.T.; Appi, C.J.; Soldan, A.L.; Cerqueira, J.R. O neo-Alagoas nas bacias do Ceará, Araripe e Potiguar (Brasil): Caracterização estratigráfica e paleoambiental. *Rev. Bras. Geociênc.* **1987**, *17*, 118–122. [CrossRef]
52. Neumann, V.H.M.L. Estratigrafía, Sedimentología, Geoquímica y Diagénesis de los Sistemas Lacustres Aptienses-Albienses de la Cuenca de Araripe (Noreste de Brasil). Ph.D Thesis, University of Barcelona, Barcelona, Spain, 1999.
53. Oliveira, G.R.; Kellner, A.W. Rare hatchling specimens of Araripemys Price, 1973 (Testudines, Pelomedusoides, Araripemydidae) from the Crato Formation, Araripe Basin. *J. South. Am. Earth Sci.* **2017**, *79*, 137–142. [CrossRef]
54. Filho, E.B.D.S.; Adami-Rodrigues, K.; De Lima, F.J.; Bantim, R.A.M.; Wappler, T.; Saraiva, A. Álamo, F. Evidence of plant–insect interaction in the Early Cretaceous Flora from the Crato Formation, Araripe Basin, Northeast Brazil. *Hist. Biol.* **2017**, *31*, 926–937. [CrossRef]

55. Osés, G.L.; Petri, S.; Voltani, C.G.; Prado, G.; Galante, D.; Rizzutto, M.A.; Rudnitzki, I.D.; Da Silva, E.P.; Rodrigues, F.; Rangel, E.; et al. Deciphering pyritization-kerogenization gradient for fish soft-tissue preservation. *Sci. Rep.* **2017**, *7*, 1–15. [CrossRef] [PubMed]
56. Catto, B.; Jahnert, R.J.; Warren, L.V.; Varejao, F.G.; Assine, M.L. The microbial nature of laminated limestones: Lessons from the Upper Aptian, Araripe Basin, Brazil. *Sediment. Geol.* **2016**, *341*, 304–315. [CrossRef]
57. Warren, L.V.; Varejão, F.G.; Quaglio, F.; Simoes, M.; Fürsich, F.T.; Poiré, D.G.; Catto, B.; Assine, M. Stromatolites from the Aptian Crato Formation, a hypersaline lake system in the Araripe Basin, northeastern Brazil. *Facies* **2016**, *63*, 3. [CrossRef]
58. Nascimento, D.R., Jr.; da Silva Filho, W.F.; Freire, J.G., Jr.; dos Santos, F.H. Syngenetic and diagenetic features of evaporite-lutite successions of the Ipubi Formation, Araripe Basin, Santana do Cariri, NE Brazil. *J. S. Am. Earth Sci.* **2016**, *72*, 315–327. [CrossRef]
59. Martill, D.M. Preservation of Fish in the Cretaceous Santana Formation of Brazil. *Palaeontology* **1988**, *31*, 1–18.
60. Fara, E.; Saraiva, A.Á.F.; Campos, D.D.A.; Moreira, J.K.; Siebra, D.D.C.; Kellner, A.W. Controlled excavations in the Romualdo Member of the Santana Formation (Early Cretaceous, Araripe Basin, northeastern Brazil): Stratigraphic, palaeoenvironmental and palaeoecological implications. *Palaeogeogr. Palaeoclim. Palaeoecol.* **2005**, *218*, 145–160. [CrossRef]
61. Kellner, A.W.A.; Campos, D.A. Brief review of dinosaur studies and perspectives in Brazil. *Anais Acad. Brasil. Ciênc.* **2000**, *72*, 509–538. [CrossRef] [PubMed]
62. Romano, P.S.R.; Oliveira, G.R.; Azevedo, S.A.K.; Kellner, A.W.A.; Campos, D.D.A. New Information about Pelomedusoides (Testudines: Pleurodira) from the Cretaceous of Brazil. In *Morphology and Evolution of Turtles*; Springer: Berlin, Germany, 2013; pp. 261–275.
63. Custódio, M.A.; Quaglio, F.; Warren, L.V.; Simões, M.G.; Fürsich, F.T.; Perinotto, J.A.J.; Assine, M. The transgressive-regressive cycle of the Romualdo Formation (Araripe Basin): Sedimentary archive of the Early Cretaceous marine ingression in the interior of Northeast Brazil. *Sediment. Geol.* **2017**, *359*, 1–15. [CrossRef]
64. Chagas, D.B.; Assine, M.L.; Freitas, F.I. Fácies Sedimentares e ambientes deposicionais da Formação Barbalha no Vale do Cariri, Bacia do Araripe, Nordeste do Brasil. *Geociências* **2007**, *26*, 313–322.
65. Chagas, D.B. Análise Faciológica Frente ao Controle Paleoambiental Baseado na Palinologia do Intervalo Aptiano/Albiano da Bacia do Araripe (Sub-Bacias Cariri e Feira Nova), NE do Brasil. Ph.D. Thesis, Federal University of Ceará, Fortaleza, CE, Brazil, 2017.
66. Reis, D.E.S.; Caputo, M.V. Potencial industrial e energético do folhelho pirobetuminoso Formação Codó, Bacia do Parnaíba. In Proceedings of the 4° PDPETRO, Campinas, SP, Brazil, 21–24 October 2007; pp. 1–10.
67. Peters, K.E.; Cassa, M.R.; Magoon, L.B.; Dow, W.G. Applied Source Rock Geochemistry. In *The Petroleum System—From Source to Trap*; American Association of Petroleum Geologists AAPG/Datapages: Tulsa, OK, USA, 1994; Volume 60, pp. 93–120.
68. Espitalié, J.; Laporte, J.L.; Madec, M.; Marquis, F.; Leplat, P.; Paulet, J.; Boutefeu, A. Méthode rapide de caractérisation des roches mètres, de leur potentiel pétrolier et de leur degré d'évolution. *Rev. Inst. Fr. Pétrole* **1977**, *32*, 23–42. [CrossRef]
69. Bordenave, M.L.; Espitalié, J.; Leplat, P.; Oudin, J.L.; Vandenbroucke, M. Screening Techniques for Source Rock Evaluation. In *Applied Petroleum Geochemistry*; Bordenave, M.L., Ed.; Editions Technip: Paris, France, 1993; ISBN 978-271-080-629-5.
70. Espitalie, J.; DeRoo, G.; Marquis, F. La pyrolyse Rock-Eval et ses applications. Deuxième partie. *Rev. Inst. Fr. Pétrole* **1985**, *40*, 755–784. [CrossRef]
71. Tissot, B.P.; Welte, D.H. *Petroleum Formation and Occurrence*; Springer Science & Business Media: Berlin, Germany, 1984; Part II, Chapter 1; ISBN 364-287-813-X.
72. Berner, R.A.; Raiswell, R. Burial of organic carbon and pyrite sulfur in sediments over phanerozoic time: A new theory. *Geochim. Cosmochim. Acta* **1983**, *47*, 855–862. [CrossRef]
73. Leventhal, J.S. Carbon-sulfur plots to show diagenetic and epigenetic sulfidation in sediments. *Geochim. Cosmochim. Acta* **1995**, *59*, 1207–1211. [CrossRef]
74. Raiswell, R. Chemical Models of Solute Acquisition in Glacial Melt Waters. *J. Glaciol.* **1984**, *30*, 49–57. [CrossRef]
75. Woolfe, K.J.; Dale, P.J.; Brunskill, G.J. Sedimentary C/S relationships in a large tropical estuary: Evidence for refractory carbon inputs from mangroves. *Geo Mar. Lett.* **1995**, *15*, 140–144. [CrossRef]
76. Arthur, M.A.; Brumsack, H.-J.; Jenkyns, H.; Schlanger, S.O. Stratigraphy, Geochemistry, and Paleoceanography of Organic Carbon-Rich Cretaceous Sequences. *Cret. Res. Events Rhythm.* **1990**, 75–119. [CrossRef]
77. Koutsoukos, E.A.M.; Mello, M.R.; Filho, N.C.D.A. Micropalaeontological and geochemical evidence of mid-Cretaceous dysoxic-anoxic palaeoenvironments in the Sergipe Basin, northeastern Brazil. *Geol. Soc. Lond. Spec. Publ.* **1991**, *58*, 427–447. [CrossRef]
78. Begon, M.; Towsend, C.R.; Harper, J.L. *Ecologia: De Indivíduos a Populações*, 4th ed.; Artmed: Porto Alegre, RS, Brazil, 2007; ISBN 978-853-630-884-5.
79. Warren, J.K. *Evaporites: Sediments, Resources and Hydrocarbons*, 1st ed.; Springer Science & Business Media: Berlin, Germany, 2006; p. 1036. ISBN 978-3-540-32344-0.
80. Katz, B.J. Factors Controlling the Development of Lacustrine Petroleum Source Rocks—An Update. In *Paleogeography, Paleoclimate, and Source Rocks*; American Association of Petroleum Geologists AAPG/Datapages: Tulsa, OK, USA, 1995; ISBN 978-162-981-087-4.
81. Wefer, G.; Berger, W.H.; Bijma, J.; Fischer, G. *Clues to Ocean. History: A Brief. Overview of Proxies*; Springer Science and Business Media LLC: Berlin, Germany, 1999; pp. 1–68.

82. Price, L.I. A presença de Pterosauria no Cretáceo Inferior da Chapada do Araripe, Brasil. *Anais Acad. Bras. Ciênc.* **1971**, *43*, 451–461.
83. Martill, D.M. The significance of the Santana Biota. In Proceedings of the Atas do I Simposio sobre a Bacia do Araripe e Bacias Interiores do Nordeste, Crato, CE, Brazil, 14–16 June 1990; pp. 253–264.
84. Bruno, A.D.S.; Hessel, M.H. Registros paleontológicos do Cretáceo marinho na Bacia do Araripe. *Estudos Geol.* **2006**, *16*, 30–49.
85. Farina, M. Seqüência plumbífera do Araripe-mineralização sulfetada no Cretáceo sedimentar brasileiro. In Proceedings of the Congresso Brasileiro de Geologia, Porto Alegre, RS, Brazil, 24–26 October 1974; pp. 61–77.
86. Rios-Netto, A.D.M.; Regali, M.D.S.P.; Carvalho, I.D.S.; De Freitas, F.I. Palinoestratigrafia do intervalo Alagoas da Bacia do Araripe, Nordeste do Brasil. *Rev. Bras. Geociênc.* **2012**, *42*, 331–342. [CrossRef]
87. Lima, M.R. Considerações sobre a subdivisão estratigráfica da Formação Santana—Cretáceo do Nordeste do Brasil. *Rev. Bras. Geociênc.* **1979**, *9*, 116–121.
88. Arai, M.; Coimbra, J.C. Análise paleoecológica do registro das primeiras ingressões marinhas na Formação Santana (Cretáceo Inferior da Chapada do Araripe). In Proceedings of the Simpósio sobre a Bacia do Araripe e Bacias Interiores do Nordeste, Crato, CE, Brazil; 1990; pp. 225–239.
89. Assine, M.L. Análise estratigráfica da bacia do araripe, nordeste do Brasil. *Rev. Bras. Geociênc.* **1992**, *22*, 289–300. [CrossRef]
90. Claypool, G.E.; Holser, W.T.; Kaplan, I.R.; Sakai, H.; Zak, I. The age curves of sulfur and oxygen isotopes in marine sulfate and their mutual interpretation. *Chem. Geol.* **1980**, *28*, 199–260. [CrossRef]
91. Sharp, Z. *Principles of Stable Isotope Geochemistry*, 2nd ed.; The University of New Mexico: Albuquerque, NM, USA, 2017; p. 344.
92. Faure, G. *Principles of Isotope Geology*; John Wiley & Sons: Hoboken, NJ, USA, 1977; p. 464. ISBN 978-047-125-665-6.
93. Kaplan, I.R.; Rittenberg, S.C. Microbiological Fractionation of Sulphur Isotopes. *J. Gen. Microbiol.* **1964**, *34*, 195–212. [CrossRef]
94. Bottrell, S.H.; Newton, R.J. Reconstruction of changes in global sulfur cycling from marine sulfate isotopes. *Earth Sci. Rev.* **2006**, *75*, 59–83. [CrossRef]
95. Böttcher, M.E.; Lepland, A. Biogeochemistry of sulfur in a sediment core from the west-central Baltic Sea: Evidence from stable isotopes and pyrite textures. *J. Mar. Syst.* **2000**, *25*, 299–312. [CrossRef]
96. Fry, B.; Jannasch, H.W.; Molyneaux, S.J.; Wirsen, C.O.; Muramoto, J.A.; King, S. Stable isotope studies of the carbon, nitrogen and sulfur cycles in the Black Sea and the Cariaco Trench. *Deep. Sea Res. Part A Oceanogr. Res. Pap.* **1991**, *38*, S1003–S1019. [CrossRef]
97. Neretin, L.N.; Böttcher, M.E.; Grinenko, V.A. Sulfur isotope geochemistry of the Black Sea water column. *Chem. Geol.* **2003**, *200*, 59–69. [CrossRef]
98. Barros, S.D.S.; Horn, B.L.D.; Santos, R.B.; Rocha, D.E.G.A. Geoquímica isotopic na reconstrução paleoambiental da Formação Ipubi (Porção superior do Grupo Santana Pós-rifte I) Bacia do Araripe Noroeste do Estado de Pernambuco. In Proceedings of the Anais Congresso Brasileiro de Geologia—48, Porto Alegre, RS, Brazil, 24–28 October 2016; p. 1034.
99. Berner, R.A. Burial of organic carbon and pyrite sulfur in the modern ocean; its geochemical and environmental significance. *Am. J. Sci.* **1982**, *282*, 451–473. [CrossRef]
100. Berner, R.A. Sedimentary pyrite formation: An update. *Geochim. Cosmochim. Acta* **1984**, *48*, 605–615. [CrossRef]
101. Fleurance, S.; Cuney, M.; Malartre, F.; Reyx, J. Origin of the extreme polymetallic enrichment (Cd, Cr, Mo, Ni, U, V, Zn) of the Late Cretaceous–Early Tertiary Belqa Group, central Jordan. *Palaeogeogr. Palaeoclim. Palaeoecol.* **2013**, *369*, 201–219. [CrossRef]
102. Coimbra, J.C.; Arai, M.; Carreño, A.L. Biostratigraphy of Lower Cretaceous microfossils from the Araripe basin, northeastern Brazil. *Geobios* **2002**, *35*, 687–698. [CrossRef]
103. Neumann, V.; Borrego, A.; Cabrera, L.; Dino, R. Organic matter composition and distribution through the Aptian–Albian lacustrine sequences of the Araripe Basin, northeastern Brazil. *Int. J. Coal Geol.* **2003**, *54*, 21–40. [CrossRef]
104. Tomé, M.E.; Filho, M.F.L.; Neumann, V.H. Taxonomic studies of non-marine ostracods in the Lower Cretaceous (Aptian–lower Albian) of post-rift sequence from Jatobá and Araripe basins (Northeast Brazil): Stratigraphic implications. *Cretac. Res.* **2014**, *48*, 153–176. [CrossRef]
105. Varejão, F.G.; Silva, V.R.; Assine, M.L.; Warren, L.V.; Matos, S.A.; Rodrigues, M.G.; Fürsich, F.T.; Simões, M.G. Marine or freshwater? Accessing the paleoenvironmental parameters of the Caldas Bed, a key marker bed in the Crato Formation (Araripe Basin, NE Brazil). *Braz. J. Geol.* **2021**, *51*. [CrossRef]
106. Heimhofer, U.; Hochuli, P.-A. Early Cretaceous angiosperm pollen from a low-latitude succession (Araripe Basin, NE Brazil). *Rev. Palaeobot. Palynol.* **2010**, *161*, 105–126. [CrossRef]
107. Varejão, F.G.; Warren, L.V.; Simões, M.G.; Buatois, L.A.; Mángano, M.G.; Rumbelsperger, A.M.B.; Assine, M.L. Mixed siliciclastic–carbonate sedimentation in an evolving epicontinental sea: Aptian record of marginal marine settings in the interior basins of north-eastern Brazil. *Sedimentology* **2021**. [CrossRef]
108. Garcia, G.G.; Garcia, A.J.V.; Henriques, M.H.P. Palynology of the Morro do Chaves Formation (Lower Cretaceous), Sergipe Alagoas Basin, NE Brazil: Paleoenvironmental implications for the early history of the South Atlantic. *Cretac. Res.* **2018**, *90*, 7–20. [CrossRef]
109. Lúcio, T.; Neto, J.A.S.; Selby, D. Late Barremian/Early Aptian Re–Os age of the Ipubi Formation black shales: Stratigraphic and paleoenvironmental implications for Araripe Basin, northeastern Brazil. *J. S. Am. Earth Sci.* **2020**, *102*, 102699. [CrossRef]
110. Coimbra, J.C.; Freire, T.M. Age of the Post-rift Sequence I from the Araripe Basin, Lower Cretaceous, NE Brazil: Implications for spatio-temporal correlation. *Rev. Bras. Paleontol.* **2021**, *24*, 37–46. [CrossRef]

111. Martill, D.M.; Brito, P.M.; Donovan, S.K. There are rudists in Brazil! Derived examples of cf. Amphitriscoelus Harris and Hodson, 1922, in the Araripe Basin, north-east Brazil: Implications for dating of the fossil Lagerstätten of the Santana and Crato formations. *Cretac. Res.* **2021**, *120*, 104718. [CrossRef]
112. Jenkyns, H.C. Geochemistry of oceanic anoxic events. *Geochem. Geophys. Geosyst.* **2010**, *11*. [CrossRef]